A Wavelet Transform for Atrial Fibrillation Cycle Length Measurements

R Dubois[1], P Roussel[1], M Hocini[2], F Sacher[2],
M Haissaguerre[2], G Dreyfus[1]

[1]Laboratoire d'Electronique, ESPCI-ParisTech, Paris, France
[2]Hopital Cardiologique du Haut-Lévèque, Université Victor Segalen, Bordeaux II, France

Abstract

We describe a new algorithm for the estimation of Cycle Lengths (CL) in the atria. In the spirit of wavelet transforms, the algorithm correlates the electrogram (EGM) signal to a set of functions that are specifically designed to extract the cycle length present in the signal on a given time window. This provides a CL vs time map, which is a highly informative representation of the electrical activation of the tissue. Subsequently, the information from this map is compressed into a histogram that unravels the distribution of the dominant CLs.. Finally, a sliding window tracks automatically the changes in CLs over a larger time scale. Results on both synthetic and real data are presented. The correlation with known cycle lengths in the synthetic cases is strong, and the CL distributions on real data are similar to those obtained from manually annotated EGMs.

1. Introduction

Catheter ablation is a common treatment for atrial fibrillation. During the procedure, endocardial electrograms (EGM) are recorded in various locations of the atria and analyzed by the physician in order to decide whether ablation must be performed or not. Traditionally, the mean cycle length is extracted from EGMs as an estimate of the mean duration between two consecutive activations in the tissue. It turned out to be a valuable guideline during the procedure: when measured in a fixed location (coronary sinus or left appendage for example) its value greatly increases after the ablation of a site involved in sustaining the atrial fibrillation (AF), and conversely, does not change after the ablation of an inactive site [1].

During the procedure, the CL is usually computed from a bipolar filtered signal. More recently, the value of the CL was correlated to the dominant frequency of the signal; therefore, the Fourier Transform is also used now [2-4].

In this paper, we present a new wavelet-like algorithm for the estimation of the Cycle Lengths (CL) in the atria. Section II describes the generation of time *vs* CL maps, and their transformation into a histogram to exhibit the dominant CLs on a given time window. In section III, comparison with Fast Fourier Transform is first presented on synthetic signal, and results on real data are compared to manually annotated EGMs. Results are discussed in the final section.

2. Methods

2.1. Wavelet transforms

The wavelet transform is based on the computation of the inner product of a function with shifted and scaled versions of a 'mother' function. Very frequently, the mother functions are oscillatory in nature, so that dilations result in frequency changes, and shifts result in time shifts; the values of the correlations computed in given time and frequency ranges are usually plotted in the form of a time-frequency map.

In the present work, we focus on cycle lengths instead of frequencies; therefore, we design a "mother function" Φ_N that is suitable for our purpose, and we compute the correlation function of a signal $x(t)$ with the mother function as $C_N(T) = \int_{-\infty}^{+\infty} x(t)\Phi_N(t+T)dt$, expressing the similarity between signal x and the mother function. Therefore, in order to avoid using the term 'mother function' too loosely, it will be termed 'template function' in the following.

2.2. Template function

The template function used here is equal to the sum of two identical Gaussian functions separated by N ms (Figure 1):

$$\Phi_N(t) = \exp\left(-\frac{(t-N/2)^2}{2\sigma^2}\right) + \exp\left(-\frac{(t+N/2)^2}{2\sigma^2}\right)$$

The width σ is fixed and the time interval N between

the Gaussians is a parameter.

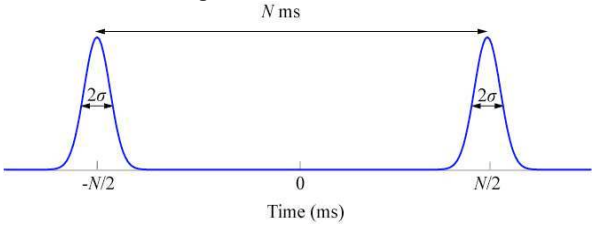

Figure 1: Mother function used for CL measurement.

Let s be an EGM signal. The correlation between its power s^2 and the i-th template function, with parameter N_i, is thus given by:

$$C_{N_i}(T) = \int_{-\infty}^{+\infty} s^2(t)\,\Phi_{N_i}(t+T)\,dt$$

It can be written as:

$$C_{N_i}(T) = G(T - N_i/2) + G(T + N_i/2)$$

where $G(T)$ is the correlation function of the signal s^2 and the Gaussian function ($-T$, σ):

$$G(u) = \int_{-\infty}^{+\infty} s^2(t)\exp\left(-\frac{(t+u)^2}{2\sigma^2}\right)dt$$

Thus, if the spikes in $s(t)$ are identical, the value of C_{Ni} is maximum when $G(T - N_i/2)$ and $G(T + N_i/2)$ are simultaneously maximum. This occurs when the time interval between two consecutive depolarisations of the tissue are separated by a time interval of N_i ms. i.e. when the cycle length is equal to N_i. Consequently, the values of N_i chosen for the analysis are equal to the values of CLs to be analyzed, Φ_{N_i} being specific of a CL of N_i ms.

In usual cases, a set of 101 template functions is used, corresponding to cycle lengths in the range 120-220 ms with a 1ms resolution. The decomposition over the whole basis can be represented as a CL *vs.* time map where the values along the *z*-axis represent the values of coefficients C_N (Figure 2).

2.3. From CL *vs* time maps to CL detection

In order to obtain a global picture of the cycle length contents of the signal, the maximum values of C_N are computed for each N on a time window of size I:

$$M_I(N) = \max_{T \in I} C_N(T)$$

A local maximum of M_I at N_i corresponds to the presence of that particular CL in the signal during the time window I, the value of that maximum being proportional to the energy generated by the corresponding depolarization. Typically, the length of I is chosen equal to 500 ms (Figure 2, bottom right).

2.4. CL tracking

The computation of the $M_I(N)$ on a sliding window allows the tracking of the CLs over a large time window W. A new map composed of each M_I curve is then displayed. This map is a highly informative description of the pattern of cycle lengths during the time window W: changes, appearances or disappearances of CLs are displayed clearly in such a representation (Figure 3). The synthesis of this map is obtained by analyzing the local maxima of each M_I curve; a histogram is finally obtained by counting the number of occurrences of each CL. This histogram, can be seen as the probability distribution of the CLs over the time window W.

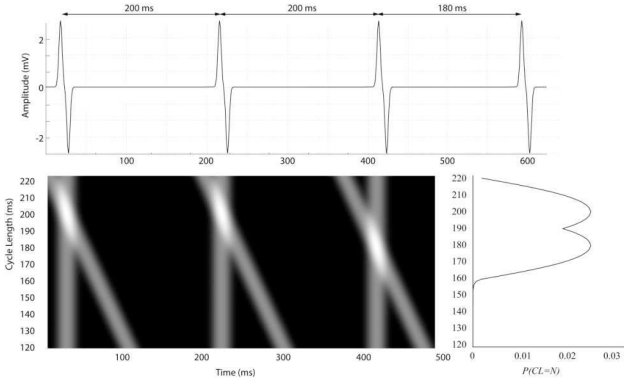

Figure 2: (Top) Synthetic EGM with three known CLs: 200 ms for the first two CLs and 180 ms for the third one. (Bottom left) Values of $C_N(T)$ for N between 120 ms and 220 ms in a 500 ms time interval. High values (in white) correspond to the onset of a cycle at a given time: the first two white spots correspond to the onsets of the first two 200 ms cycles and the third one to the onset of a 180 ms cycle. (Bottom right) M_I curve extracted from the map. The two local maxima correspond to the two values of CLs of the signal: 180 ms and 200 ms.

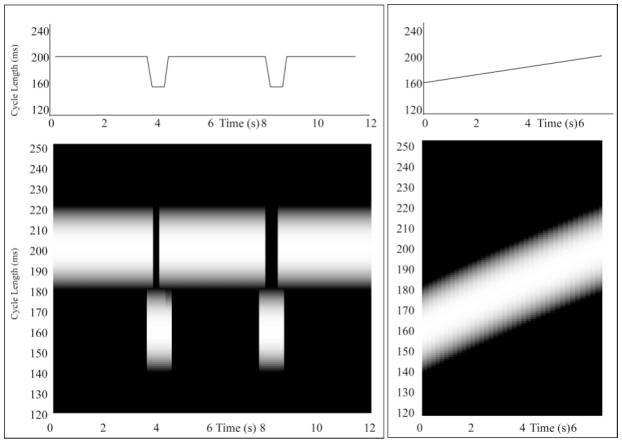

Figure 3: (Left panel) Result obtained on a synthetic 12s signal that has a fixed CL at 200 ms and two burst of 8 depolarizations at 160 ms. (Right panel) Result obtained on a synthetic signal exhibiting CLs of increasing length, from 160ms to 200ms every 1ms.

3. Results

The performance of this method is first compared to existing algorithms (Dominant Frequency and autocorrelation) on synthetic EGMs with known cycle lengths. In the third subsection, results on real data pertaining to 7 patients who underwent RF-catheter ablation for AF are presented.

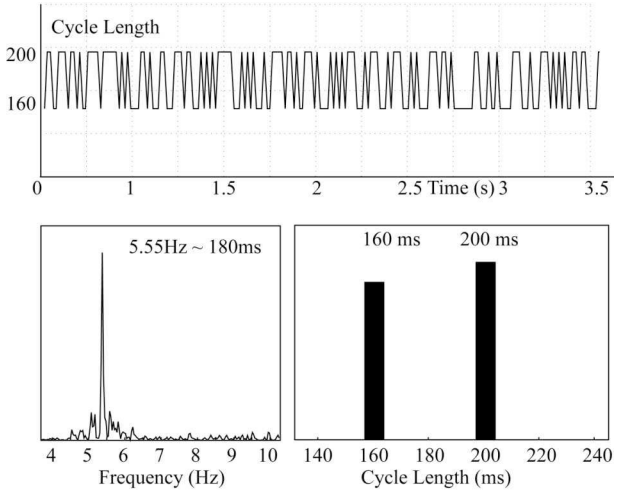

Figure 4: (Top) Value of CLs for a synthetic signal exhibiting randomly alternating depolarizations at 160ms and 200ms. (Bottom Left) Corresponding spectrum: the DF is 5.12Hz (i.e. 195 ms). (Bottom right) Application of our method to the same signal: two CLs are detected at 160 ms and 200ms.

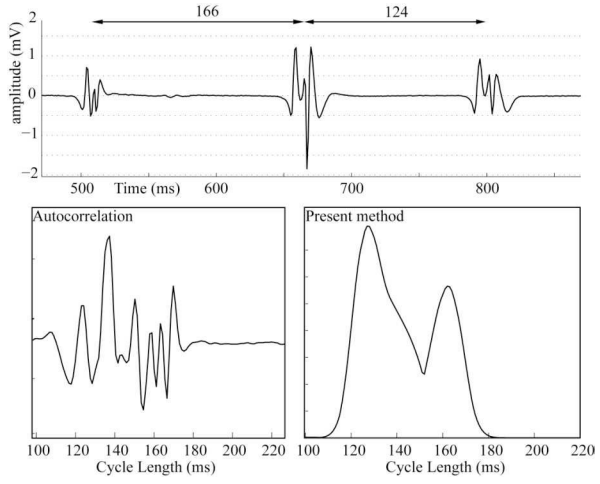

Figure 5: Data recorded in the left appendage for a persistent AF case. The autocorrelation function results in several peaks due to the complexity of the signal. The $M_I(N)$ function computed over the same window exhibits only two peaks around the two values of CLs of the signal. The broadening of the peaks results from the fragmentation of the signal.

3.1. Comparison with Dominant Frequency

The dominant frequency method for CL detection is based on a spectral analysis of the EGM signal over a time window *I*. After a preprocessing step (filtering and rectification), a Fast Fourier Transform is computed. It has been shown that the highest peak in the frequency domain (dominant frequency) is related to the mean CL of the signal over the time window *I* [2-4]. This method was shown to be efficient in particular for fragmented EGM, but some issues limit its use [5-6]. For example, a theoretical issue arises when two separate focal sources randomly alternate 160ms and 200ms CLs. The DF computed from the FFT analysis is linked to the mean frequency of the two sources. Figure 4 illustrates this property; on this synthetic example, the DF is 5.12Hz (195 ms). This value lies between 160 ms and 200 ms. The method proposed above leads to a histogram showing clearly the two expected values, 160 and 200ms.

3.2. Comparison with autocorrelation

The computation of the autocorrelation has been proposed for the evaluation of the CLs. This method was shown to be efficient especially for monophasic action potentials. But, in the case of a fragmented signal, the estimation of the CL seems difficult (Figure 5).

3.3. Results on real data

The algorithm efficiency was estimated on 7 patients with drug-refractory AF. AF was paroxysmal in 3 patients, persistent in 2 and permanent in 2.

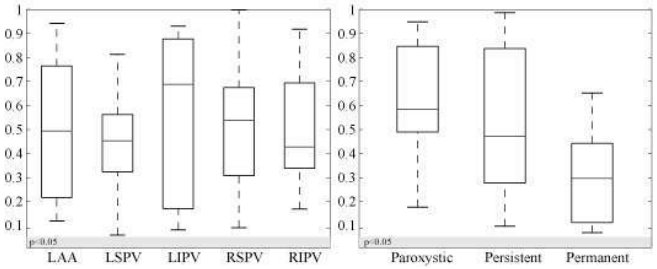

Figure 6: *p*-values obtained with the Chi-squared contingency test for distribution comparison between manually labeled CLs and automatically annotated CLs for AF. All *p* values are greater than 0.05, thereby supporting the null hypothesis that the two sets of measurements arise from the same distribution. (Left) The *p*-values are presented by location. On each box, the central mark is the median, the edges of the box are the 25th and 75th percentiles, the whiskers extend to the most extreme data points. (Right) The results are presented for each pathology, unlike the graph by location, the median value of *p* increases with the pathology seriousness.

EGM was recorded prior to any ablation within the left atrium using a 10 bipole mapping catheter for at least 30 seconds in the following sites: Left Appendage (LAA), Left Superior (LSPV), Left Inferior (LIPV), Right Superior (RSPV) and Right Inferior (RIPV) pulmonary veins. For each site, a single EGM was selected from the 10 available signals from signal to noise ratio considerations. CLs were manually measured for each selected signal to serve as a reference. On the same signals, CLs were estimated with the proposed algorithm on 500 ms sliding windows, every 250 ms, and CL histograms were compared to the reference with a Chi-squared contingency test, the null hypothesis being that the two measurements have identical continuous distributions: the test shows that the null hypothesis cannot be rejected under standard risk assumption of 0.05 (i.e. $p < 0.05$) for all EGMs (Figure 6).

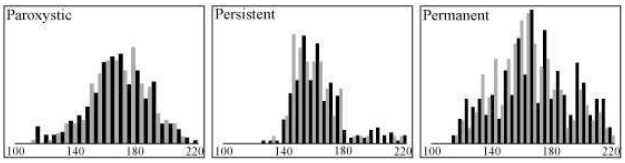

Figure 7: Histogram of the estimated CL distribution (gray) and reference CL distribution (black) for the three median values of p.

4. Conclusions and discussion

The proposed algorithm extracts the CL efficiently on both synthetic and real data. The correlation with known cycle lengths in the synthetic cases is strong, and this method is shown to be efficient for burst detection and multiple CL recognition. On real data, the CLs obtained with this method are similar to those obtained from manually annotated EGMs, especially in paroxystic AF. In addition, the results does not depend on the measurement site: the median of CL in each location are almost the same (Figure 6-left). But, the higher the complexity of AF is, the greater is the error between reference and automatic annotation on the results (Figure 6-right). A possible explanation for this result is that in persistent AF cases, the depolarisations are usually fragmented and manually positioning single markers is more subjective (Figure 7).

The method requires the adjustement of some parameters. In the results presented here, the width of the Gaussian function was set to 5ms, which is the mean duration of a non-fragmented depolarization. The influence of this parameter appears in the computation of G, which results in a Gaussian smoothing of the signal. Its value should be large enough to smooth the signal in order to avoid double counting for a single depolarization, but small enough to obtain a good resolution in CLs. Secondly, the size I of the time window has been set to 250 ms. This value guarantees that at least two subsequent depolarizations of the tissue can be observed. Since the CL information from CL v*s*. time maps are condensed by estimating the maximum over this time window I (see section 2.3), a larger window should be considered only if the signal is stable.

Furthermore, this method provides highly informative maps that characterize the EGM, and some parameters can be extracted from this representation: for example, stability can be estimated by the width of the peaks (Figure 5). Activation maps between different location of the atria prior to any ablation can be also compared in order to select site of interest. But the efficiency as a guideline for ablation is still to be investigated. A strategy could be to correlate the complexity of a map at a given location prior to ablation to the increase of the CL after ablation at that location.

References

[1] Haissaguerre M, Sanders P, Hocini M, Hsu L-F, Shah DC, Scavee C, et al. Changes in Atrial Fibrillation Cycle Length and Inducibility During Catheter Ablation and Their Relation to Outcome. Circulation. 2004 June 22, 2004;109(24):3007-13.

[2] Everett TH, Lai-Chow K, Vaughn RH, Moorman RA, Haines DE. Frequency domain algorithm for quantifying atrial fibrillation organization to increase defibrillation. IEEE Trans Biomedical Engineering. 2001;48(9):969-78.

[3] Sanders P, Nalliah CJ, Dubois R, Takahashi Y, Hocini M, Rotter M, et al. Frequency Mapping of the Pulmonary Veins in Paroxysmal Versus Permanent Atrial Fibrillation. Journal of Cardiovascular Electrophysiology. 2006;17(9):965-72.

[4] Takahashi Y, Sanders P, Dubois R, Rotter M, Rostock T, Hocini M, et al., editors. Dynamic Changes in Spatial Periodicity of Dominant Frequency in Left Atrium. Heart Rhythm; 2005.

[5] Narayan SM, Franz MR. Quantifying fractionation and rate in human atrial fibrillation using monophasic action potentials: implications for substrate mapping. Europace. 2007 Nov;9:89-95.

[6] Ng J, Kadish AH, Goldberger JJ. Effect of electrogram characteristics on the relationship of dominant frequency to atrial activation rate in atrial fibrillation. Heart Rhythm. 2006;3(11):1295-305.

Address for correspondence:
Rémi Dubois
Lab d'Électronique
ESPCI-ParisTech
10 rue Vauquelin
75005 Paris, France.

E-mail address: remi.dubois@espci.fr